Biomacromolecules

Article

Cite This: Biomacromolecules 2019, 20, 4191−4198

pubs.acs.org/Biomac

Electrospinning Nanofibers from Chitosan/Hyaluronic Acid Complex Coacervates

Juanfeng Sun, Sarah L. Perry,* and Jessica D. Schiffman*

Department of Chemical Engineering, University of Massachusetts Amherst, Amherst, Massachusetts 01003, United States

Supporting Information

ABSTRACT: Electrospun biopolyelectrolyte nanofibers hold potential for use in a range of biomedical applications, but eliminating toxic chemicals involved in their production remains a key challenge. In this study, we successfully electrospun nanofibers from an aqueous complex coacervate solution composed of chitosan and hyaluronic acid. Experimentally, we investigated the effect of added salt and electrospinning apparatus parameters, such as how applied voltage affected fiber formation. We also studied how the addition of alcohol cosolvents affected the properties of the coacervate solution and the resulting nanofibers. Overall, we observed a trade-off in how the addition of salt and alcohol affected the phase behavior and rheology of the coacervates and, consequently, the size of the resulting fibers. While salt served to weaken electrostatic associations within the coacervate and decrease the precursor solution viscosity, the addition of alcohol lowered the dielectric constant of the system and strengthened these interactions. We hypothesize that the optimized concentration of alcohol accelerated the solvent evaporation during the electrospinning process to yield desirable nanofiber morphology. The smallest average nanofiber diameter was determined to be 115 ± 30 nm when coacervate samples were electrospun using an aqueous solvent containing 3 wt % ethanol and an applied voltage of 24 kV. These results demonstrate a potentially scalable strategy to manufacture electrospun nanofibers from biopolymer complex coacervates that eliminate the need for toxic solvents and could enable the use of these materials across a range of biomedical applications.

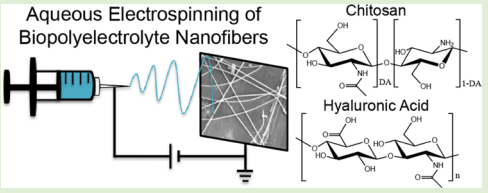

INTRODUCTION

Electrospinning is a facile technique used to produce continuous polymer fiber mats with diameters ranging from the nano- to the micrometer scale.[1,2] The outstanding properties of electrospun fiber mats, including their high porosity and large surface-to-volume ratio, make these nanomaterials excellent for use in medical applications,[3−5] such as artificial organs,[5] tissue scaffolds,[6−8] drug delivery,[3,5,6,9−11] and wound dressings.[4,5,9−11] In particular, fibrous mats composed of biopolyelectrolytes, such as chitosan and hyaluronic acid, hold great promise for use in biomedicine due to their low toxicity and high biocompatibility. It has been suggested that fibers composed of chitosan and hyaluronic acid hold potential as an improved wound-healing matrix.[12−17]

Chitosan is a cationic polysaccharide composed of 2-acetamide-2-deoxy-β-D-glucopyranose and 2-amino-2-deoxy-β-D-glucopyranose (Figure 1a).[14−16] Much of the utility of chitosan in medical applications has come from its hemostatic properties.[14,16,17] Hyaluronic acid is also a polysaccharide that carries a single negative charge for each pair of α-1,4-D-glucuronic acid and β-1,3-N-acetyl-D-glucosamine disaccharide units (Figure 1a), which has demonstrated healing properties.[12,18−20]

One of the major challenges of electrospinning charged polymers, including cationic chitosan and anionic hyaluronic acid, has been the need to prepare a polymer solution at a high enough concentration (i.e., above the critical entanglement concentration) such that the physical entanglements between polymer chains can stabilize the formation of a continuous fiber.[14,21−24] Repulsive interactions between like-charged groups along the polymer backbone cause the viscosity of aqueous solutions of charged polymers to increase dramatically with increasing polymer concentration, hindering the electrospinning process.[9,14,16,21−23,25−29] To date, the utility of pure chitosan fibers has been limited because they have only been electrospun using highly concentrated acidic solutions, which raise concerns about the biocompatibility of the final product.[14,26−29] Typically, chitosan-based fibers have been electrospun by blending weakly acidic chitosan solutions with a neutral polymer, such as poly(ethylene oxide).[14,18,19,30] Electrospinning precursor solutions containing the anionic polymer hyaluronic acid also require the use of organic solvents, blending with a neutral polymer, or supplemental air flow.[20,24,31−34] While these strategies have facilitated the preparation of an entangled solution with viscosities that can be electrospun, such approaches can diminish the efficacy (i.e., the ability to produce the desired result) of the biomaterial because less of the functional polymer is included in the final product.[14,18,24] Additionally, mats electrospun from either chitosan or hyaluronic acid require cross-linking to improve their chemical stability.[20,24−27,31,32,34,35]

Received: August 2, 2019
Revised: October 13, 2019
Published: October 15, 2019

DOI: 10.1021/acs.biomac.9b01072
Biomacromolecules 2019, 20, 4191−4198

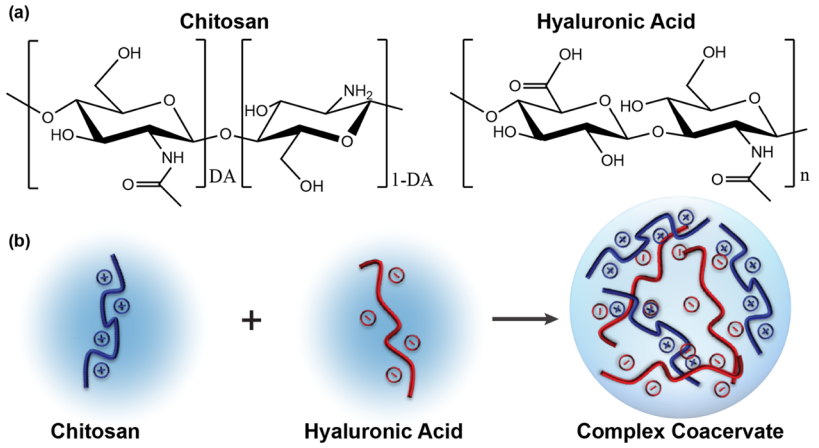

Figure 1. (a) Molecular structures of chitosan and hyaluronic acid. The degree of acetylation (DA) of chitosan is the fractional number of acetylglucosamine units in the polymer. (b) Schematic depiction of complex coacervation resulting from the interaction and liquid−liquid phase separation of oppositely charged polyelectrolytes in water.

Our team recently reported an alternative strategy to enable the electrospinning of stable fibers from an aqueous mixture of oppositely charged polymers that takes advantage of a liquid−liquid phase separation phenomenon known as complex coacervation (Figure 1b).[36] Complex coacervation is an electrostatic and entropically driven phase separation that results in the formation of a dense, polymer-rich coacervate phase in equilibrium with a polymer-poor supernatant.[37−42] The phase behavior and rheological character of complex coacervates can be influenced by various parameters, such as ionic strength, pH value, stoichiometry, polymer chain length, charge density, and polymer chemistry.[37−44] The complex coacervation of chitosan and hyaluronic acid has been reported previously[44,45] and represents a potential strategy for electrospinning because of the favorable properties of the individual biopolymers. However, the electrospinning of biopolymer-based coacervates introduces additional chemical and physical complexities that, to date, have not been studied. In particular, the deacetylation of chitin is known to result in blocky charged and neutral regions along the polymer,[17,46,47] the effect of which has not been tested in the context of electrospinning complex coacervate precursor solutions. Our goal is to explore if complex coacervates formed from commercially purchased chitosan, hyaluronic acid, and sodium chloride can be electrospun into nanofiber mats.

To date, there are a very limited number of reports on fabricating nanofibers that contain two oppositely charged polymers. While previous groups have fabricated electrospun fibers that contained two oppositely charged polymers, this has been achieved through postprocessing or via an experimental design that alters the charge state of one of the polymers during or after the spinning process.[48−51] For instance, fibers containing chitosan and hyaluronic acid have been prepared by first electrospinning chitosan alone, followed by a separate coating step to incorporate hyaluronic acid onto the fibers.[12] In contrast, Penchev et al. were able to electrospin a single-phase solution of chitosan and poly(acrylic acid) (PAA) using formic acid at a low pH value to eliminate the negative charge on the acid groups.[52] The two polymers were then able to form a polyelectrolyte complex during the spinning process as the volatilization of the formic acid increased the local pH value within the fibers. The same report also described the use of a ternary solvent system to facilitate the spinning of chitosan with a strong polyacid. In this case, the authors hypothesized that the combination of organic solvent and salt helped to balance out interactions and eliminate complexation. Boas et al.[53] reported a similar approach that used pH value and an ethanol cosolvent to eliminate the charge on the PAA and allow for weaker complexation via hydrogen bonding. Finally, a third approach made use of a complex dual-spinneret setup, as well as the inclusion of polyethylene oxide to decrease the precursor solution viscosity.[54] Unfortunately, these reports all feature process limitations, including the need for overnight cross-linking at high temperatures, reliance on organic solvents, more complex apparatus setups, and/or postprocessing.[48−51]

Here, we employ thermodynamically driven liquid−liquid phase separation to create a spinnable precursor solution directly from aqueous solutions of chitosan and hyaluronic acid. Employing complex coacervates as an electrospinning precursor solution results in several improvements over previously electrospun biopolyelectrolytes: (i) the fibers are electrospun without requiring toxic solvents or carrier polymers, (ii) a simple single-syringe electrospinning setup is employed, (iii) fiber mats are completely composed of the charged biopolymers, chitosan, and hyaluronic acid, and (iv) we eliminate the need for cross-linking during or after electrospinning. This work explores the feasibility and process parameters required to electrospin biopolyelectrolyte nanofiber mats from aqueous solutions.

EXPERIMENTAL SECTION

Materials. Chitosan with a degree of deacetylation in the range of 75−85% and an average molecular weight of 50−190 kDa (Sigma-Aldrich) was dissolved in a solution that was adjusted to have a pH value of 4.5 before being filtered through a 0.45 μm pore size filter (Millipore Express). Sodium hyaluronate with an average molecular weight of 199 kDa (Lifecore Biomedical) was dissolved in a solution that had a pH value of 4.5 before being filtered using a 0.22 μm pore size filter (Millipore Express). Sodium chloride (NaCl, ACS-grade), hydrochloric acid (HCl), sodium hydroxide (NaOH), methanol, ethanol, as well as aqueous buffers (pH = 4.0, 7.0, and 10.0) were used as received from Fisher Scientific. Deionized water was obtained from a Barnstead Nanopure Infinity water purification system (Thermo Fisher Scientific).

Chitosan/Hyaluronic Acid Complex Coacervate Preparation and Characterization. Stock solutions of chitosan and hyaluronic acid were prepared gravimetrically at 60 mM on a chargeable monomer basis (i.e., the concentration of chitosan was adjusted to

DOI: 10.1021/acs.biomac.9b01072
Biomacromolecules 2019, 20, 4191−4198

take into account the fraction of deacetylated groups, resulting in solution concentrations of 13.4 mg/mL or 1.34 w/v% chitosan and 22.8 mg/mL or 2.28 w/v% hyaluronic acid). An aqueous solution of 5 M NaCl was prepared gravimetrically, and all solutions were adjusted to pH 4.5 by adding concentrated HCl or NaOH. Complex coacervates were prepared by first combining the NaCl solution with water in a Falcon round-bottom tube (14 mL, Fisher Scientific), followed by methanol or ethanol (0, 3, 5, 8 wt %). Chitosan and hyaluronic acid were then added sequentially (in a 1:1 charge ratio unless otherwise specified) at a total chargeable monomer concentration of 40 mM (i.e., 12.1 mg/mL or 1.21 w/v% polymer). The mixture was vortexed for 10 s immediately after the addition of each solution to ensure complete mixing. After coacervate formation, samples were then centrifuged (Sorvall Legend X1r Centrifuge, Thermo Fisher Scientific) at 2000 rpm for 15 min to separate the dense coacervate phase.

Samples for turbidity and optical microscopy were prepared using the same method described above but at a smaller scale (120 μL) and a total polymer concentration of 1 mM monomer (i.e., 0.30 mg/mL or 0.03 w/v% polymer). Immediately after their preparation, three 35 μL aliquots of each sample were pipetted into a 384-well plate (Falcon). Turbidity measurements were performed using a microplate reader (BioTek Synergy H1) at a wavelength of 562 nm. Samples were then inspected visually using optical microscopy (EVOS XL Core) to confirm the presence or absence of phase separation, as well as the liquid or solid nature of complexes that might have formed.

The rheological properties of the complex coacervates were determined using small-amplitude oscillatory shear measurements on a Malvern Kinexus Pro stress-controlled instrument. Strain amplitude measurements were first conducted to determine the appropriate strain rate to use within the linear viscoelastic region. Next, frequency sweeps were conducted over the range of frequencies from 100 to 1 (rad/s). Chitosan/hyaluronic acid coacervates prepared at 300−600 mM NaCl were studied using a 20 mm diameter stainless steel parallel plate fixture with a solvent trap, whereas a 50 mm 2° core-and-plate fixture was used for samples prepared at 700 mM NaCl. Duplicate experiments were conducted. All data analysis was conducted using IRIS software (Interactive Rheology Information Systems Development LLC).[55]

Electrospinning and Characterization of Chitosan/Hyaluronic Acid Coacervate Nanofibers. Coacervates were loaded into a 5 mL syringe (Henke Sass Wolf, Norm-Ject Luer Lock) capped with a PrecisionGlide 22-gauge needle (Becton, Dickinson & Co.). The syringe was secured to a PHD Ultra syringe pump (Harvard Apparatus). Alligator clips were used to connect the positive anode of a high-voltage supply (γ High Voltage Research Inc.) to the needle and the negative anode to a copper plate covered with aluminum foil. For all experiments, the coacervate precursor solution was advanced at a constant rate of 1.0 mL/h, and the needle-to-collector separation distance was held constant at 12 cm, while the applied voltage was systematically varied (18, 20, 22, and 24 kV). The electrospinning apparatus was housed in an environmental chamber (CleaTech) that was maintained at a constant temperature of 24 ± 1 °C and a relative humidity of 23−25% using a desiccant unit (Drierite).

Fiber morphology was examined using a scanning electron microscope (SEM, FEI-Magellan 400). All SEM samples were sputter-coated for 180 s with gold (Cressington high-resolution ion beam coater model 108). Fiber diameter was determined using Image J 1.80 software (National Institutes of Health) by measuring the diameter of 30 different fibers from high-resolution SEM micrographs.

RESULTS AND DISCUSSION

The goal of this work was to explore the electrospinnability of complex coacervates formed from the biopolymers chitosan and hyaluronic acid. We explored (i) how changes in solution conditions affected the phase behavior of the resulting liquid coacervates and/or solid polyelectrolyte complexes, (ii) how these changes translated to the rheological character of the precursor coacervate solution, and (iii) how these trends correlated with electrospinnability. While our previous reports utilized complex coacervates formed from the strong polyelectrolytes poly(4-styrene sulfonic acid sodium salt) (PSS) and poly(diallyldimethylammonium chloride) (PDADMAC),[36] the charges on these polymers were uniformly distributed. In contrast, the deacetylation of chitosan is known to result in blocky charged and neutral regions along the polymer that could potentially affect the self-assembly and/or the rheological properties of the resulting coacervates.[17,46,47] Additionally, the charged nature of both hyaluronic acid and chitosan is pH-dependent. Kayitmazer et al. reported pK_a values for hyaluronic acid in the range of 2.4−2.9, as a function of polymer molecular weight, and a pK_a for chitosan of 6.4.[44] Based on these results and the molecular weight of our polymers, we elected to operate at a solution pH of 4.5. This value is halfway between the apparent pK_a values of the two polymers and is approximately two pH units away from the pK_a of each of the polymers. Thus, we used the simplifying assumption that all of the available charged groups on each polymer were charged.

Turbidity was used to qualitatively track complex formation as a function of the charge stoichiometry and salt concentration of the sample. The data in Figure 2 shows a maximum turbidity signal at a charge fraction of 0.5, corresponding to a 1:1 mixture of positively and negatively charged groups. This result supports the idea that the two polymers were fully charged at a pH value of 4.5. Interestingly, both the charge stoichiometry and the ionic strength of the solution dictated the solid vs. liquid nature of the resulting complexes. At 200 mM NaCl, only solid complexes formed. However, at 600 mM NaCl, complex coacervation (i.e., liquid−liquid phase separation) was observed for stoichiometries in the range from 0.4 to 0.6 (Figure 2, red shaded area), whereas solid complexes were observed at lower and higher ratios.

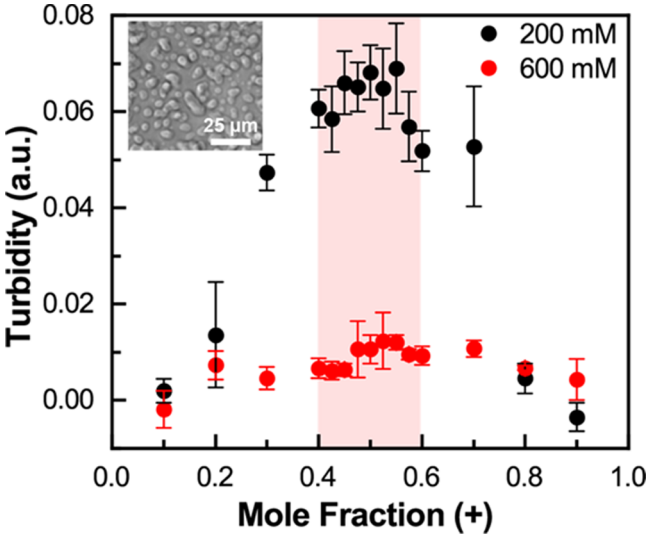

Figure 2. Turbidity as a function of the mole fraction of cationic groups from chitosan for chitosan/hyaluronic acid coacervates at different salt concentrations. The red shaded region indicates the range of mole fractions where liquid coacervates were observed at 600 mM NaCl. The inset optical micrograph displays a sample at a 0.5 mole fraction (+) at 600 mM NaCl. All samples were prepared at a 1 mM total monomer concentration at pH 4.5.

DOI: 10.1021/acs.biomac.9b01072
Biomacromolecules 2019, 20, 4191−4198

Our observation of solid polyelectrolyte complexes occurring at low salt concentration and the transition to liquid complex coacervates at higher ionic strength (shown schematically in Figure 3a) has been previously reported for a range of

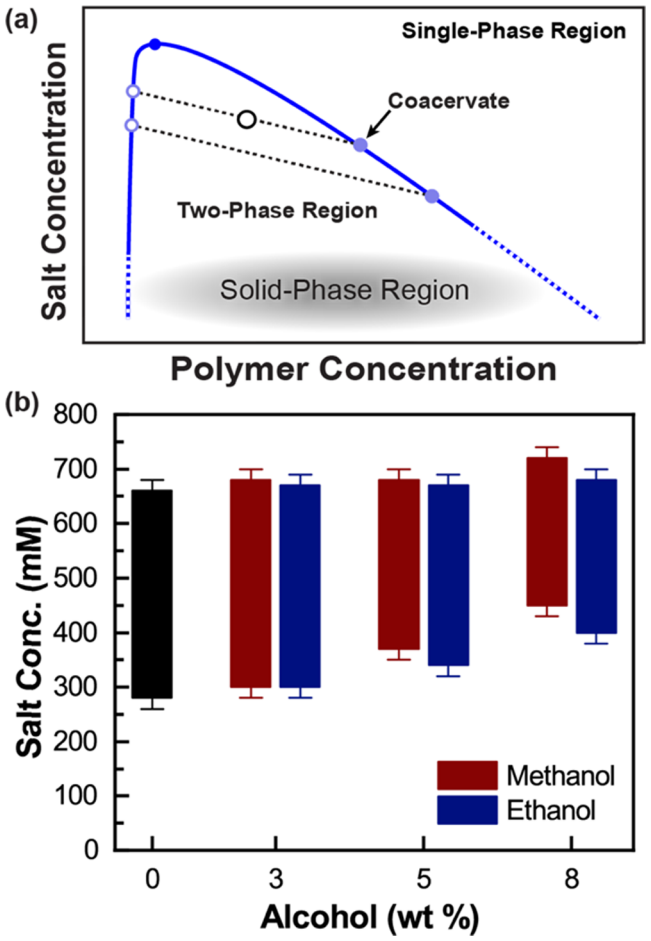

Figure 3. (a) Schematic representation of the thermodynamic phase diagram for complex coacervation as a function of salt and polymer concentration (at a given temperature, polymer composition, pH, etc.). A sample prepared at a concentration within the two-phase region beneath the phase boundary will separate along tie-lines into a polymer-rich complex coacervate phase and a polymer-poor supernatant. While the liquid coacervate phase represents the equilibrium phase transition, kinetically trapped solid polyelectrolyte complexes can occur at lower salt concentrations. (b) Liquid coacervation was observed over the displayed range of salt concentrations for 1:1 (mol/mol) complexes of chitosan and hyaluronic acid as a function of alcohol concentration, from 0 to 8 wt %. Above this range of salt, no phase separation was observed, and below this range of salt, solid precipitates formed. All samples were prepared at a 1 mM total chargeable monomer concentration at pH 4.5.

polyelectrolytes.[36−40,55,56] This type of reversible solid-to-liquid transition has been characterized as physical gelation, whereby the ionic interactions between polymers that drive complex coacervation become trapped and unable to rearrange due to the removal of salt and water.[55] Based on optical microscopy, we observed this transition from solid precipitates to liquid coacervates at 280 mM NaCl. Additionally, no phase separation was observed above a concentration of 660 mM NaCl (Figure 3b).

Having identified the range of salt concentrations over which liquid coacervates could be formed, we then attempted to electrospin fibers. Interestingly, we were able to successfully electrospin continuous, cylindrical nanofibers from aqueous chitosan/hyaluronic acid coacervates prepared at 600 mM NaCl. Continuous fibers were first observed at an applied voltage of 18 kV (Figure 4). SEM micrographs showed that the

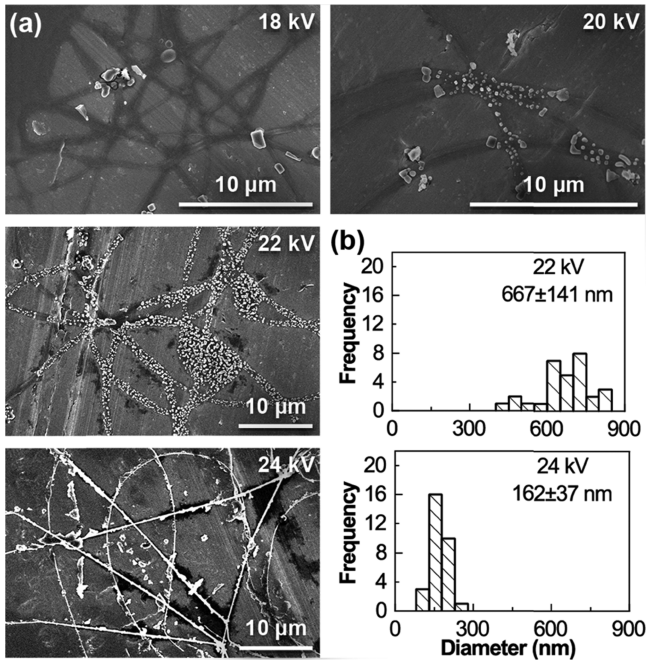

Figure 4. SEM micrographs of chitosan/hyaluronic acid fibers electrospun from aqueous complex coacervates prepared at 600 mM NaCl and pH 4.5 as a function of the applied voltage. (b) Fiber diameter distributions for successfully formed fibers. The applied voltage used, as well as the average fiber diameter and standard deviation, is indicated.

fibers had a smooth fiber morphology and possible webbing, along with the presence of salt crystals and hydrogel-like fibers. This is consistent with the previous reports on electrospinning hydrophilic biopolyelectrolytes.[33] In contrast, fibers electrospun at 24 kV were more cylindrical and significantly smaller (an average diameter of 162 ± 37 nm for fibers prepared at 24 kV compared to that of 667 ± 141 nm for fibers prepared at 22 kV; Figure 4). This trend is consistent with literature reports that increasing the applied voltage results in thinner fibers at a fixed distance from spinneret to collector.[36,57,58]

In comparison with our previous experience electrospinning the strong and synthetic polyelectrolytes PSS/PDADMAC, chitosan/hyaluronic acid coacervates required higher applied voltages and spun within a narrower range of salt concentrations.[36] These observations, coupled with the observation of the more hydrogel-like fibers formed from the biopolyelectrolytes, inspired us to explore strategies to modulate the electrostatic interactions within our precursor coacervates to potentially improve the morphology of the electrospun fibers. To this end, we investigated how the addition of small quantities of solvents with higher volatility than water would affect coacervate formation and fiber formation.

With respect to coacervate phase behavior, the addition of a miscible cosolvent would be expected to affect the electrostatic interactions within the coacervate based on the resulting change in the overall solvent dielectric constant. The dielectric

DOI: 10.1021/acs.biomac.9b01072
Biomacromolecules 2019, 20, 4191−4198

constant for methanol, ethanol, and isopropanol is lower than that of water and decreases with increasing alkyl chain length (Table S1). With increasing alcohol concentration, we observed a shift in the range of salt concentrations over which coacervation occurred. The minimum salt concentration needed to achieve liquid−liquid phase separation, as opposed to solid precipitation, increased from 280 to 400 mM NaCl with the addition of 8 wt % methanol and further increased to 450 mM NaCl in the presence of the same quantity of ethanol (Figure 3). We also observed an increase in the concentration of salt above which no phase separation was observed, although the magnitude of the change was smaller. We were unable to obtain liquid coacervates upon the addition of more than 5 wt % isopropanol. Estimation of the dielectric constant of the resulting cosolvent mixtures suggests that liquid coacervation may be disfavored for conditions where the dielectric constant falls below ~70 (Table S2). However, we cannot say for certain if this is purely an electrostatic effect or the result of other interactions, such as increased hydrogen bonding between the biopolymers.

We hypothesized that the addition of small amounts of alcohol to our coacervates would facilitate electrospinning by strengthening the cohesiveness of the precursor solution while accelerating solvent evaporation during the electrospinning process. Experimentally, we were able to obtain smooth, continuous fibers in the presence of ethanol (Figure 5). The

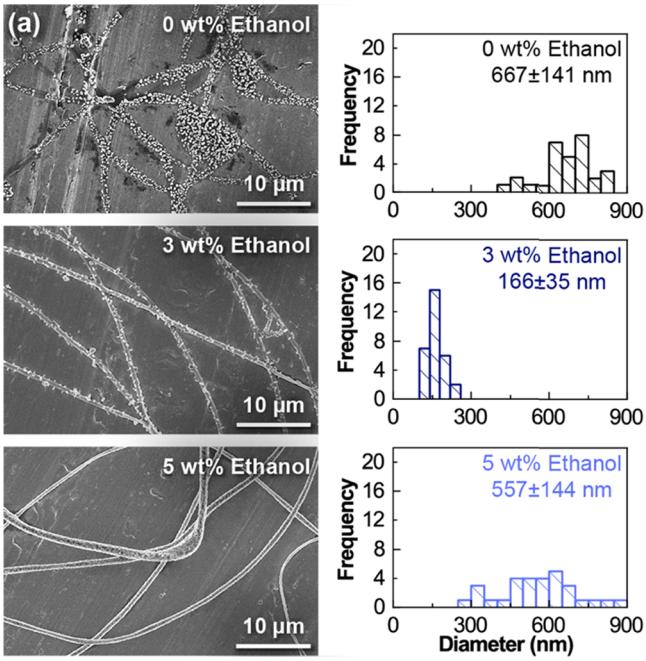

Figure 5. (a) SEM micrographs and (b) fiber diameter distribution for chitosan/hyaluronic acid fibers electrospun from aqueous complex coacervates containing 0, 3, and 5 wt % ethanol, as well as 600 mM NaCl, pH 4.5. The average fiber diameter and standard deviation are indicated. A micrograph of 8 wt % ethanol is available in Figure S1.

addition of 3 wt % ethanol resulted in a decrease in the fiber diameter compared to that of the fully aqueous case (166 ± 35 vs 667 ± 141 nm). However, at 5 wt % ethanol, we observed an increase in the fiber diameter to 557 ± 144 nm. No fiber formation was observed at 8 wt % ethanol. We posit that the initial decrease in the fiber diameter was due to improved solvent evaporation, while the subsequent increase in the diameter and loss of fiber formation was due to the increased viscosity of the coacervate precursor solution. Consistent with previous reports,[36,57,58] increasing the applied voltage decreased the diameter of the resulting fibers (Figure 6).

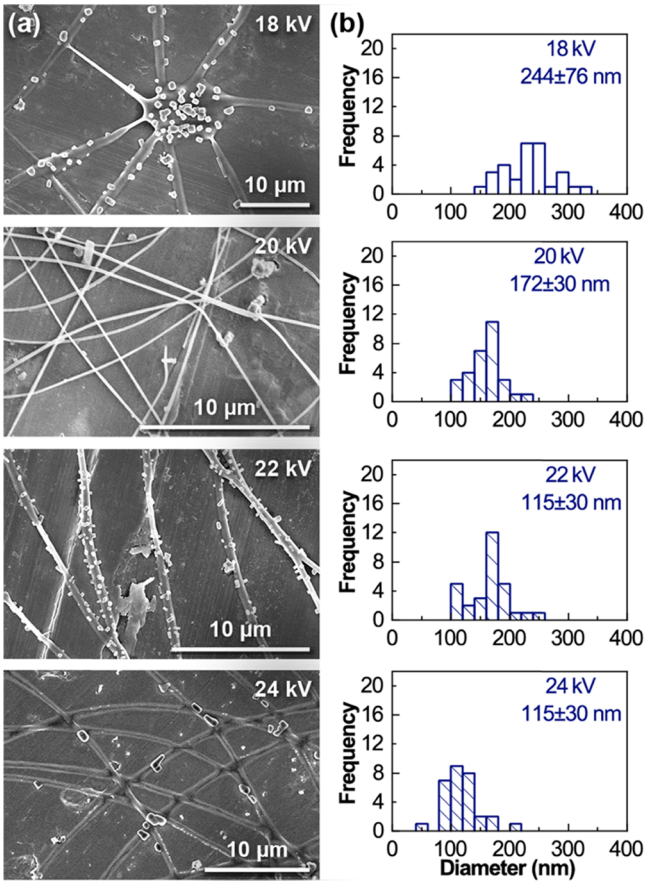

Figure 6. (a) SEM micrographs and the (b) fiber diameter distribution for chitosan/hyaluronic acid fibers electrospun from aqueous complex coacervates containing 3 wt % ethanol, as well as 600 mM NaCl, pH 4.5. The applied voltage and average fiber diameter and standard deviation are indicated.

We next turned to rheological measurements as a strategy for understanding the effect of both salt and alcohol on the spinnability of our chitosan/hyaluronic acid complex coacervates. Coacervates prepared at the lowest salt concentration of 300 mM NaCl had the highest overall modulus and showed a linear viscoelastic response that was dominated by the storage modulus (G') over the entire frequency range. As expected, we observed a decrease in the magnitude of the storage (G') and loss (G'') moduli with increasing salt concentration (Figure 7).[36,45] Along with this decrease in the overall modulus, we observed the presence of a crossover point between G' and G'' that shifted to higher frequencies with increasing salt concentration. This shift in the crossover point, along with the corresponding dominance of the loss modulus (G''), indicates that coacervates prepared at higher salt concentrations relax faster and behave in a more liquid-like manner. This salt-induced relaxation has been described as a decrease in the friction between oppositely charged polymers[36,47] and could similarly be considered as a weakening of the electrostatic interactions between polymers.

DOI: 10.1021/acs.biomac.9b01072
Biomacromolecules 2019, 20, 4191−4198

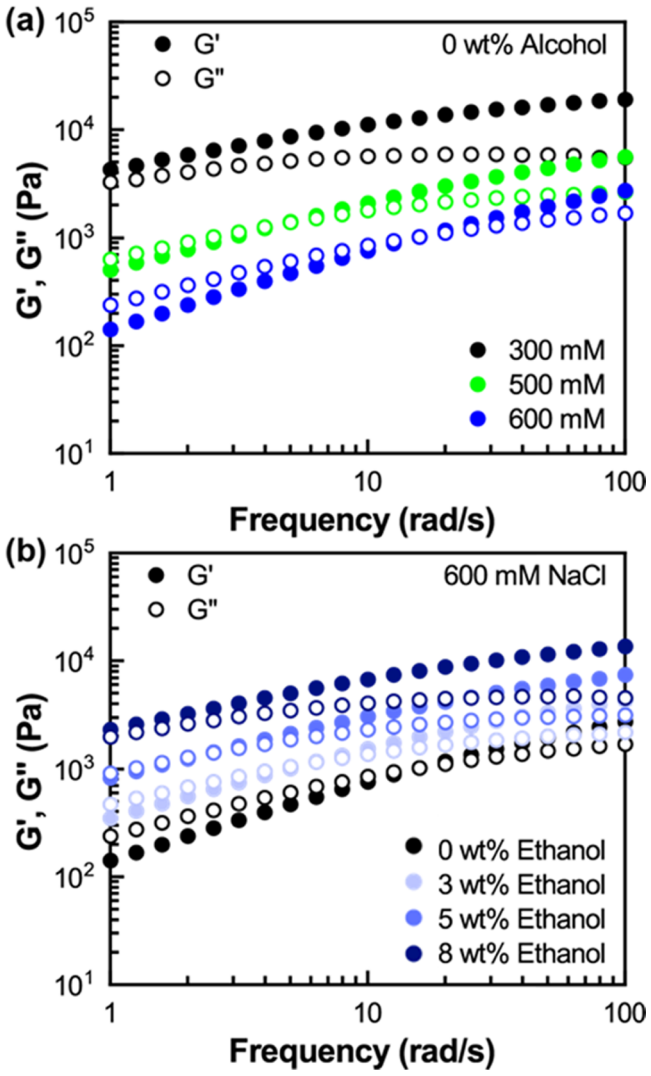

Figure 7. Frequency sweep data for (a) aqueous samples prepared at different concentrations of NaCl and (b) 600 mM NaCl samples at different concentrations of ethanol. Additional data at different salt, ethanol, and/or methanol concentrations are available in Figures S2–S4.

A similar trend of increasing modulus and slower relaxation was observed with increasing alcohol concentration (Figures 7b and S2–S4). Here, rather than the salt facilitating chain rearrangement, we hypothesize that the decreased dielectric constant of the solvent mixtures hindered relaxation by strengthening the electrostatic attractions between the oppositely charged groups on the polymers, as per Coulomb's law. These results raise the possibility of using salt concentration and cosolvent concentration as two independent handles for tuning the properties of the coacervate itself, as well as the resulting electrospun fibers.

Figure 8 shows a plot of zero-shear viscosity as a function of salt concentration for coacervates in the presence of increasing weight percent alcohol. As would be expected, the viscosity decreased with increasing salt concentration and increased with increasing alcohol concentration. A direct comparison between the data for ethanol and methanol suggests relatively similar effects, with methanol having a slightly weaker effect on the viscosity. Furthermore, we can use Figure 8 to identify conditions that allow for the preparation of coacervates with

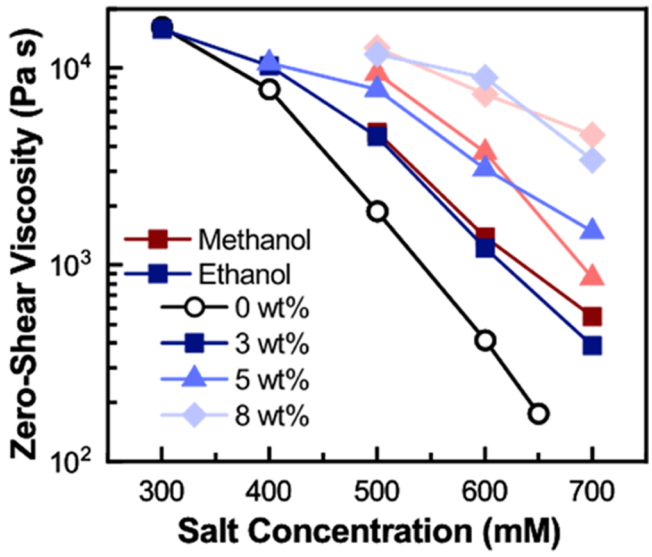

Figure 8. Plot of the zero-shear viscosity of chitosan/hyaluronic acid coacervates as a function of salt and methanol or ethanol concentration.

the same viscosity but different compositions. For instance, coacervates prepared in water at 400 mM NaCl show nearly identical viscosity as samples prepared at 500 mM NaCl and 5 wt % ethanol.

These data also suggest potential explanations for the electrospinnability of the various coacervate samples. Fibers were successfully electrospun from coacervates prepared in ethanol/water mixtures over the range of 400–600 mM NaCl at concentrations from 0 to 5 wt % ethanol. However, we observed a potential transition in the spinnability at 600 mM when 8 wt % ethanol was tested; here, bending instabilities did not occur during the flight path from the syringe to the collector plate, resulting in the deposition of one larger fiber. The same phenomenon was observed with methanol. We were able to electrospin 0–5 wt % methanol-containing coacervates at 600 mM NaCl, but consistent nanofiber mats were not spun from 8 wt % methanol coacervates (Figure S1).

From an engineering heuristics perspective, it is interesting to speculate about defining a rule of thumb that could guide coacervate formulation that would subsequently lead to spinnable precursor solutions. For our system, the effect of increasing the salt concentration by 100 mM appears to be roughly counterbalanced by the addition of approximately 5 wt % alcohol. Understanding the fundamental interplay between salt and cosolvent effects is beyond the scope of the current study but represents an interesting strategy for enabling the tailored creation of designer precursor materials from first principles.

CONCLUSIONS

In summary, we have successfully electrospun fibers from chitosan/hyaluronic acid complex coacervates. Furthermore, we demonstrated the potential for cosolvent addition to modulating the phase behavior and rheology of the coacervate to facilitate electrospinning. For our system, the addition of small quantities of ethanol or methanol appeared to accelerate solvent evaporation during the electrospinning process while strengthening the cohesion of the coacervate. These contributions helped to enable the electrospinning of

DOI: 10.1021/acs.biomac.9b01072
Biomacromolecules 2019, 20, 4191–4198

cylindrical and consistent nanofibers across a broad range of electrospinning apparatus parameters. This work demonstrates the potential for using complex coacervation to facilitate the electrospinning of functional wound dressings from the biopolyelectrolytes chitosan and hyaluronic acid.

■ ASSOCIATED CONTENT

Supporting Information

The Supporting Information is available free of charge on the ACS Publications website at DOI: 10.1021/acs.biomac.9b01072.

Physical properties of the solvents used in this study (Table S1); estimated dielectric constant for cosolvent mixtures (Table S2); optical micrographs of chitosan/hyaluronic acid fibers (Figure S1); frequency sweep rheology data (Figures S2–S4) (PDF)

■ AUTHOR INFORMATION

Corresponding Authors

*E-mail: perrys@engin.umass.edu (S.L.P.).
*E-mail: schiffman@ecs.umass.edu (J.D.S.).

ORCID

Sarah L. Perry: 0000-0003-2301-6710
Jessica D. Schiffman: 0000-0002-1265-5392

Notes

The authors declare no competing financial interest.

■ ACKNOWLEDGMENTS

The authors acknowledge the support of the National Science Foundation (NSF CMMI-1727660). The authors would also like to thank Xiangxi (Zoey) Meng and Yalin Liu for helpful discussions.

■ REFERENCES

(1) Reneker, D. H.; Yarin, A. L.; Fong, H.; Koombhongse, S. Bending Instability of Electrically Charged Liquid Jets of Polymer Solutions in Electrospinning Bending Instability of Electrically Charged Liquid Jets of Polymer Solutions in Electrospinning. *J. Appl. Phys.* **2000**, *87*, 4531–4547.

(2) Palangetic, L.; Reddy, N. K.; Srinivasan, S.; Cohen, R. E.; McKinley, G. H.; Clasen, C. Dispersity and Spinnability: Why Highly Polydisperse Polymer Solutions Are Desirable for Electrospinning. *Polymer* **2014**, *55*, 4920–4931.

(3) Rieger, K. A.; Birch, N. P.; Schiffman, J. D. Designing Electrospun Nanofiber Mats to Promote Wound Healing-A Review. *J. Mater. Chem. B* **2013**, *1*, 4531–4541.

(4) Liang, D.; Hsiao, B. S.; Chu, B. Functional Electrospun Nanofibrous Scaffolds for Biomedical Applications. *Adv. Drug Delivery Rev.* **2007**, *59*, 1392–1412.

(5) Feng, Z. Q.; Leach, M. K.; Chu, X. H.; Wang, Y. C.; Tian, T.; Shi, X. L.; Ding, Y. T.; Gu, Z. Z. Electrospun Chitosan Nanofibers for Hepatocyte Culture. *J. Biomed. Nanotechnol.* **2010**, *6*, 658–666.

(6) Cui, W.; Zhou, Y.; Chang, J. Electrospun Nanofibrous Materials for Tissue Engineering and Drug Delivery. *Sci. Technol. Adv. Mater.* **2010**, *11*, 014108.

(7) Ramakrishna, S.; Fujihara, K.; Teo, W. E.; Yong, T.; Ma, Z.; Ramaseshan, R. Electrospun Nanofibers: Solving Global Issues. *Mater. Today* **2006**, *9*, 40–50.

(8) Meng, J.; Han, Z.; Kong, H.; Qi, X.; Wang, C.; Xie, S.; Xu, H. Electrospun Aligned Nanofibrous Composite of MWCNT/Polyurethane to Enhance Vascular Endothelium Cells Proliferation and Function. *J. Biomed. Mater. Res., Part A* **2010**, *95*, 312–320.

(9) Ignatova, M.; Manolova, N.; Rashkov, I. Electrospun Antibacterial Chitosan-Based Fibers. *Macromol. Biosci.* **2013**, *13*, 860–872.

(10) Son, Y. J.; Kim, W. J.; Yoo, H. S. Therapeutic Applications of Electrospun Nanofibers for Drug Delivery Systems. *Arch. Pharm. Res.* **2014**, *37*, 69–78.

(11) Engel, Y.; Schiffman, J. D.; Goddard, J. M.; Rotello, V. M. Nanomanufacturing of Biomaterials. *Mater. Today* **2012**, *15*, 478–485.

(12) Maeda, N.; Miao, J.; Simmons, T. J.; Dordick, J. S.; Linhardt, R. J. Composite Polysaccharide Fibers Prepared by Electrospinning and Coating. *Carbohydr. Polym.* **2014**, *102*, 950–955.

(13) Lallana, E.; Rios De La Rosa, J. M.; Tirella, A.; Pelliccia, M.; Gennari, A.; Stratford, I. J.; Puri, S.; Ashford, M.; Tirelli, N. Chitosan/Hyaluronic Acid Nanoparticles: Rational Design Revisited for RNA Delivery. *Mol. Pharm.* **2017**, *14*, 2422–2436.

(14) Mckee, M. G.; Wilkes, G. L.; Colby, R. H.; Long, T. E. Correlations of Solution Rheology with Electrospun Fiber Formation of Linear and Branched Polyesters. *Macromolecules* **2004**, *37*, 1760–1767.

(15) Desai, K.; Kit, K.; Li, J.; Zivanovic, S. Morphological and Surface Properties of Electrospun Chitosan Nanofibers. *Biomacromolecules* **2008**, *9*, 1000–1006.

(16) Zhang, R. Y.; Zaslavski, E.; Vasilyev, G.; Boas, M.; Zussman, E. Tunable PH-Responsive Chitosan-Poly(Acrylic Acid) Electrospun Fibers. *Biomacromolecules* **2018**, *19*, 588–595.

(17) de Farias, B. S.; Sant'Anna Cadaval Junior, T. R.; de Almeida Pinto, L. A. Chitosan-Functionalized Nanofibers: A Comprehensive Review on Challenges and Prospects for Food Applications. *Int. J. Biol. Macromol.* **2019**, *123*, 210–220.

(18) Kriegel, C.; Kit, K. M.; Mcclements, D. J.; Weiss, J. Electrospinning of Chitosan – Poly (Ethylene Oxide) Blend Nanofibers in the Presence of Micellar Surfactant Solutions. *Polymer* **2009**, *50*, 189–200.

(19) Kriegel, C.; Kit, K. M.; Mcclements, D. J.; Weiss, J. Influence of Surfactant Type and Concentration on Electrospinning of Chitosan – Poly (Ethylene Oxide) Blend Nanofibers. *Food Biophys.* **2009**, *4*, 213–228.

(20) Um, I. C.; Fang, D.; Hsiao, B. S.; Okamoto, A.; Chu, B. Electro-Spinning and Electro-Blowing of Hyaluronic Acid. *Biomacromolecules* **2004**, *5*, 1428–1436.

(21) Schiffman, J. D.; Schauer, C. L. A Review: Electrospinning of Biopolymer Nanofibers and Their Applications. *Polym. Rev.* **2008**, *48*, 317–352.

(22) Sun, K.; Li, Z. H. Preparations, Properties and Applications of Chitosan Based Nanofibers Fabricated by Electrospinning. *Express Polym. Lett.* **2011**, *5*, 342–361.

(23) Saquing, C. D.; Tang, C.; Monian, B.; Bonino, C. A.; Manasco, J. L.; Alsberg, E.; Khan, S. A. Alginate – Polyethylene Oxide Blend Nanofibers and the Role of the Carrier Polymer in Electrospinning. *Ind. Eng. Chem. Res.* **2013**, *52*, 8692–8704.

(24) Brenner, E. K.; Schiffman, J. D.; Thompson, E. A.; Toth, L. J.; Schauer, C. L. Electrospinning of Hyaluronic Acid Nanofibers from Aqueous Ammonium Solutions. *Carbohydr. Polym.* **2012**, *87*, 926–929.

(25) Vondran, J. L.; Sun, W.; Schauer, C. L. Crosslinked, Electrospun Chitosan – Poly (Ethylene Oxide) Nanofiber Mats. *J. Appl. Polym. Sci.* **2008**, *109*, 968–975.

(26) Schiffman, J. D.; Schauer, C. L. One-Step Electrospinning of Cross-Linked Chitosan Fibers. *Biomacromolecules* **2007**, *8*, 2665–2667.

(27) Schiffman, J. D.; Schauer, C. L. Cross-Linking Chitosan Nanofibers. *Biomacromolecules* **2007**, *8*, 594–601.

(28) Hasegawa, M.; Isogai, A.; Onabe, F.; Usuda, M. Dissolving States of Cellulose and Chitosan in Trifluoroacetic Acid. *J. Appl. Polym. Sci.* **1992**, *45*, 1857–1863.

(29) Hussain, T.; Masood, R.; Umar, M.; Areeb, T.; Ullah, A. Development and Characterization of Alginate-Chitosan-Hyaluronic

DOI: 10.1021/acs.biomac.9b01072
Biomacromolecules 2019, 20, 4191–4198

Acid (ACH) Composite Fibers for Medical Applications. *Fibers Polym.* **2016**, *17*, 1749−1756.
(30) Bhattarai, N.; Edmondson, D.; Veiseh, O.; Matsen, F. A.; Zhang, M. Electrospun Chitosan-Based Nanofibers and Their Cellular Compatibility. *Biomaterials* **2005**, *26*, 6176−6184.
(31) Wang, X.; Chul, I.; Fang, D.; Okamoto, A.; Hsiao, B. S.; Chu, B. Formation of Water-Resistant Hyaluronic Acid Nanofibers by Blowing-Assisted Electro-Spinning and Non-Toxic Post Treatments. *Polymer* **2005**, *46*, 4853−4867.
(32) Li, J.; He, A.; Han, C. C.; Fang, D.; Hsiao, B. S.; Chu, B. Electrospinning of Hyaluronic Acid (HA) and HA/Gelatin Blends. *Macromol. Rapid Commun.* **2006**, *27*, 114−120.
(33) Brenner, E. K.; Schiffman, J. D.; Toth, L. J.; Szewczyk, J. C.; Schauer, C. L. Phosphate Salts Facilitate the Electrospinning of Hyaluronic Acid Fiber Mats. *J. Mater Sci.* **2013**, *48*, 7805−7811.
(34) Ji, Y.; Ghosh, K.; Li, B.; Sokolov, J. C.; Clark, R. A. F.; Rafailovich, M. H. Dual-Syringe Reactive Electrospinning of Cross-Linked Hyaluronic Acid Hydrogel Nanofibers for Tissue Engineering Applications. *Macromol. Biosci.* **2006**, *6*, 811−817.
(35) Li, J.; He, A.; Zheng, J.; Han, C. C. Gelatin and Gelatin - Hyaluronic Acid Nanofibrous Membranes Produced by Electrospinning of Their Aqueous Solutions. *Biomacromolecules* **2006**, *7*, 2243−2247.
(36) Meng, X.; Perry, S. L.; Schiffman, J. D. Complex Coacervation: Chemically Stable Fibers Electrospun from Aqueous Polyelectrolyte Solutions. *ACS Macro Lett.* **2017**, *6*, 505−511.
(37) Blocher, W. C.; Perry, S. L. Complex Coacervate-Based Materials for Biomedicine. *Wiley Interdiscip. Rev.: Nanomed. Nanobiotechnol.* **2017**, *9*, e1442.
(38) Perry, S. L.; Li, Y.; Priftis, D.; Leon, L.; Tirrell, M. The Effect of Salt on the Complex Coacervation of Vinyl Polyelectrolytes. *Polymers* **2014**, *6*, 1756−1772.
(39) Liu, Y.; Winter, H. H.; Perry, S. L. Linear Viscoelasticity of Complex Coacervates. *Adv. Colloid Interface Sci.* **2017**, *239*, 46−60.
(40) Priftis, D.; Tirrell, M. Phase Behaviour and Complex Coacervation of Aqueous Polypeptide Solutions. *Soft Matter* **2012**, *8*, 9396−9405.
(41) Spruijt, E.; Westphal, A. H.; Borst, J. W.; Cohen Stuart, M. A.; Van Der Gucht, J. Binodal Compositions of Polyelectrolyte Complexes. *Macromolecules* **2010**, *43*, 6476−6484.
(42) Lytle, T. K.; Chang, L.; Markiewicz, N.; Perry, S. L.; Sing, C. E. Designing Electrostatic Interactions via Polyelectrolyte Monomer Sequence. *ACS Cent. Sci.* **2019**, *5*, 709−718.
(43) Chang, L.; Lytle, T. K.; Radhakrishna, M.; Sing, C. E.; Perry, S. L.; Madinya, J. J.; Vélez, J. Sequence and Entropy-Based Control of Complex Coacervates. *Nat. Commun.* **2017**, *8*, 1273.
(44) Kayitmazer, A. B.; Koksal, A. F.; Kilic Iyilik, E. Complex Coacervation of Hyaluronic Acid and Chitosan: Effects of PH, Ionic Strength, Charge Density, Chain Length and the Charge Ratio. *Soft Matter* **2015**, *11*, 8605−8612.
(45) Vecchies, F.; Sacco, P.; Decleva, E.; Menegazzi, R.; Porrelli, D.; Donati, I.; Turco, G.; Paoletti, S.; Marsich, E. Complex Coacervates between a Lactose-Modified Chitosan and Hyaluronic Acid as Radical-Scavenging Drug Carriers. *Biomacromolecules* **2018**, *19*, 3936−3944.
(46) Shi, R.; Sun, T. L.; Luo, F.; Nakajima, T.; Kurokawa, T.; Bin, Y. Z.; Rubinstein, M.; Gong, J. P. Elastic−Plastic Transformation of Polyelectrolyte Complex Hydrogels from Chitosan and Sodium Hyaluronate. *Macromolecules* **2018**, *51*, 8887−8898.
(47) Lalevée, G.; Sudre, G.; Montembault, A.; Meadows, J.; Malaise, S.; Crépet, A.; David, L.; Delair, T. Polyelectrolyte Complexes via Desalting Mixtures of Hyaluronic Acid and Chitosan—Physicochemical Study and Structural Analysis. *Carbohydr. Polym.* **2016**, *154*, 86−95.
(48) Penchev, H.; Paneva, D.; Manolova, N.; Rashkov, I. Novel Electrospun Nanofibers Composed of Polyelectrolyte Complexes. *Macromol. Rapid Commun.* **2008**, *29*, 677−681.
(49) Jeong, S. I.; Krebs, M. D.; Bonino, C. A.; Samorezov, J. E.; Khan, S. A.; Alsberg, E. Electrospun Chitosan−Alginate Nanofiber with In Situ Polyelectrolyte Complexation for Use as Tissue Engineering Scaffolds. *Tissue Eng., Part A* **2010**, *1*, 59−70.
(50) Chunder, A.; Sarkar, S.; Yu, Y.; Zhai, L. Fabrication of Ultrathin Polyelectrolyte Fibers and Their Controlled Release Properties. *Colloids Surf., B* **2007**, *58*, 172−179.
(51) Ma, G.; Liu, Y.; Fang, D.; Chen, J.; Peng, C.; Fei, X.; Nie, J. Hyaluronic Acid/Chitosan Polyelectrolyte Complexes Nanofibers Prepared by Electrospinning. *Mater. Lett.* **2012**, *74*, 78−80.
(52) Penchev, H.; Paneva, D.; Manolova, N.; Rashkov, I. Novel Electrospun Nanofibers Composed of Polyelectrolyte Complexes. *Macromol. Rapid Commun.* **2008**, *29*, 677−681.
(53) Boas, M.; Gradys, A.; Vasilyev, G.; Burman, M.; Zussman, E. Electrospinning Polyelectrolyte Complexs: pH-Responsive Fibers. *Soft Matter* **2015**, *11*, 1739−1747.
(54) Yuan, T. T.; Foushee, A. M. D.; Johnson, M. C.; Jockheck-clark, A. R.; Stahl, J. M. Development of Electrospun Chitosan- Polyethylene Oxide/Fibrinogen Biocomposite for Potential Wound Healing Applications. *Nanoscale Res. Lett.* **2018**, *13*, 88.
(55) Liu, Y.; Momani, B.; Winter, H. H.; Perry, S. L. Rheological Characterization of Liquid-to-Solid Transitions in Bulk Polyelectrolyte Complexes. *Soft Matter* **2017**, *13*, 7332−7340.
(56) Fares, H. M.; Ghoussoub, Y. E.; Delgado, J. D.; Fu, J.; Urban, V. S.; Schlenoff, J. B. Scattering Neutrons along the Polyelectrolyte Complex/Coacervate Continuum. *Macromolecules* **2018**, *51*, 4945−4955.
(57) Thompson, C. J.; Chase, G. G.; Yarin, A. L.; Reneker, D. H. Effects of Parameters on Nanofiber Diameter Determined from Electrospinning Model. *Polymer* **2007**, *48*, 6913−6922.
(58) Theron, S. A.; Zussman, E.; Yarin, A. L. Experimental Investigation of the Governing Parameters in the Electrospinning of Polymer Solutions. *Polymer* **2004**, *45*, 2017−2030.

DOI: 10.1021/acs.biomac.9b01072
Biomacromolecules 2019, 20, 4191−4198